



Approaches to reveal porosity in Phenolic Resin derived CFRP and C/C Composites

Herbert Mucha*, Young-Eun Kim*, Bernhard Wielage*

[Mucha]: hinoya.d@wsk.tu-chemnitz.de

*Lehrstuhl fuer Verbundwerkstoffe

Technische Universitaet Chemnitz

D-09107 Chemnitz, Germany

Keywords: *phenolic resin, carbon matrix, carbon fibers, porosity, focused ion beam*

Abstract

Phenolic resins are the first industrially produced synthetic resins (1909, Baekeland, Erkner/Germany) and widely applied in industry.

The versatile properties of phenolic resins justify their application as matrices in different kinds of composites. Some of the most important advantages are the modest price, the relative simple application (heat or acidic curing), the wide spectrum of obtainable properties and the high carbon yields. The C-yields allow the conversion of phenolic resins based Carbon Fiber Reinforced Plastics (CFRP) to high temperature C-Fiber Ceramics (C/C, C/C-SiC).

The chemistry of Carbon is the base of the phenolic resin chemistry. One of the best outlines of the empirical phenolic resin knowledge dates back to Hultzsch [1], whereas the quantum mechanical approaches are introduced e. g. by Rappoport [2].

The thermally induced transformations of the resins cause the generation of gaseous by-products and subsequently porosity. The general microstructural model of the Carbon materials is consistently applicable on the pyrolysis products.

1. The Chemistry of Phenolic Resins

The production characteristics and parameters of phenolic resins are essential for creating the particular resin character. A thermally induced generation of bridges takes place during curing and transformations start at higher temperatures. The full range of the thermal transformations can be separated in 4 steps [1]:

- 1.) Phenol-Formaldehyde-Addition Phase (15 °C- 40 °C, mono- or dimeric raw resin)
- 2.) Polymerisation phase

(60 °C - 200°C, increasing molar mass)

a.) Prepolymerisation (<100°C)
(increase of molecular mass, oligomer, retains molar mobility, no 3-dim.network, commercial material state)

b.) Final polymerization (< 200 °C)
(growth to maximum molar mass, 3-dim. network, sharply increasing viscosity, curing)

3.) Thermal transformation phase
(200 °C – 350 °C, no significant molecular size changes, bridge transformations)

4.) Cracking phase
(> 350 °C, molecular degradation, reduced molecular mass)

The observed reactivity of the phenolic system is at the first glance very surprising, specially when recalling the stability of the very similar Benzene system. But this discrepancy can be eliminated by taking the quantum mechanical point of view of the chemical bonding. Polymers are many particle systems and therefore have to be subjected to the adequate quantum mechanical formalisms /3, 4/.

The Electron Localization Function (ELF) [2] describes the electronic charge distribution in the rings (Fig.1). On ortho- and para-positions (relative to the OH-group) Phenol shows accumulated electronic charge (nucleus mantled) transferred from the OH-group (depending on their chemical loading e. g. by hydrogen bridges) into the ring. This explains why the ortho- and para-positions are more reactive as the meta-positions.

A quantum mechanical mesomer (m-) effect even allows to couple certain types of substituents to the

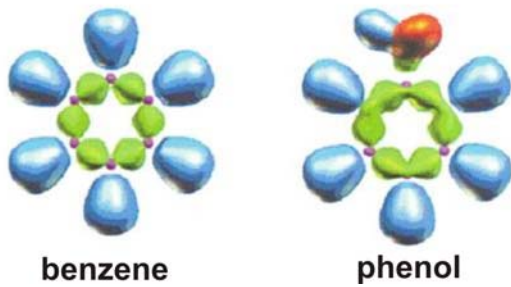


Fig. 1; Electron localization Function. (ELF) for Benzene (left) and Phenol (right), [2]

electronic charge ring system. In that case functional groups` reactivity can be controlled by the first substituent, which in Phenol is the phenolic OH-group. This effect is essential for the course of the Phenol-Formaldehyde-Addition and the polymerization phase of phenolic resins. The base of their later product properties is laid during this phase.

ELF and (m-) effect can get effective just in case a particular bonding type is provided. It is the existence of aromatic bonds (Fig. 2).

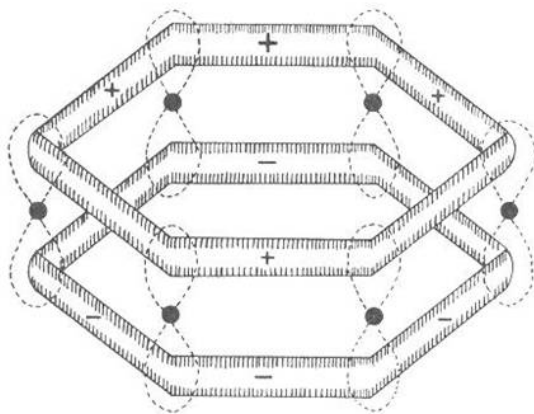


Fig. 2; π -molecular Orbital, delocalized (Benzene) [4]

The aromatic bond is distinguished by its additional π -orbital system, which is perfectly planar and delocalized. The symmetry of the arrangement, having one part above and one below the plane of atoms, causes its ideal planarity. This assertion is an outcome of the quantum mechanical treatment of the many particle system. This theory even assures that the delocalized bond type is more stable than all other bonds! Indeed the existence of aromatic bonding is an indispensable prerequisite for a material to be carbonizable. Within the general

microstructural model of the carbon materials, this fact obtains even more weight, as it allows an ab-initio interpretation of the driving forces for the graphitization of carbon materials (Fig. 3).

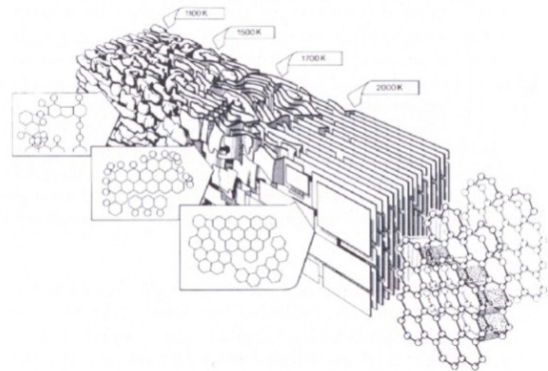


Fig. 3; Graphitization model (Marsh & Griffith), [5]

The alignment of smaller units (lower temperature) to form larger ones is accompanied with an energy reduction, if they form flat layers. Nevertheless it needs the availability of kinetic processes which facilitate these changes on the atomistic scale. In many cases the mechanisms inherent to the material are not existing or effective in unsuited temperature ranges and microstructural changes can be induced only by external influences (e. g. stretching)

The resemblance of the aromatic ring as it occurs e. g. in phenolic resins with the microstructural Basic Structural Unit (BSU) (Fig. 3) is great [6].

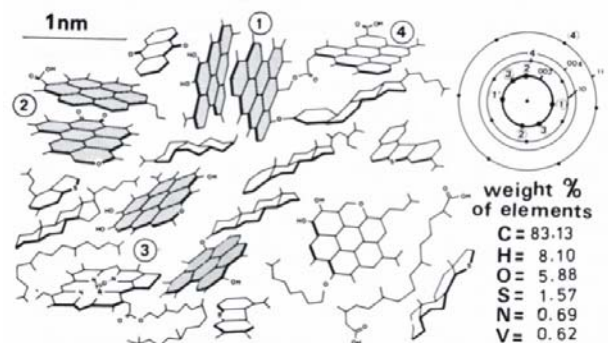


Fig. 4; The Basic Structural Units (BSU) and their Alignment in Carbon materials, Local Molecular Order, [6]

Being able to control the reactivity of the aromatic ring and the substituents by pH-value, temperature and other parameters, it is possible to set the ratio

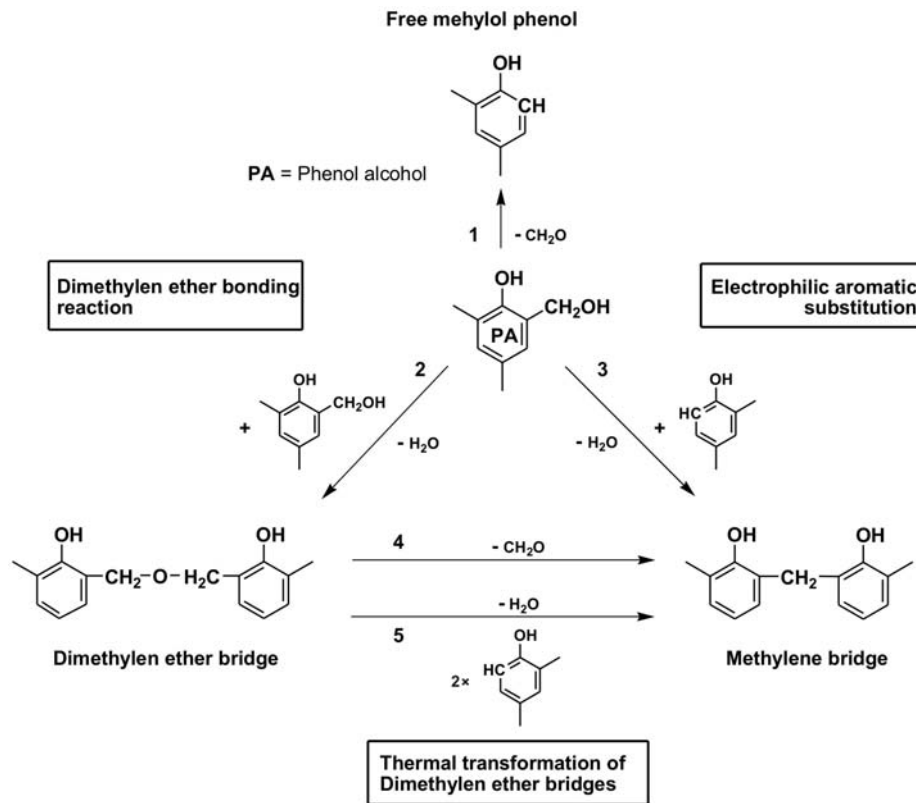


Fig. 5; Alternatives for the polymerization of phenolic resins depending on experimental boundary conditions [1]

between the Dimethylen ether bridges and the Methylene bridges. According to Hultzsich [1] the reaction paths as displayed in Fig. 5 are known. Phenolic resins can be formed as mixtures of Dimethylen Ether and Methylene bridges depending on the processing/reaction conditions. These bridges differ in their thermal stability and their content of vaporizable components, i. e. their molar ratio is a measure for their potential to create gaseous reaction products (additional to the solvent evaporation). High active phenolic resins (many methylo groups, mono- or dimer) are expected to generate more porosity as higher condensed resins (larger molar mass) can do. This interplay needs clearing by deeper investigations of the mechanisms. Knowledge about the actual chemical condition of resins will improve the reproducibility for parts fabrication.

Phenolic resins are suited to act as precursors for Carbon matrices e. g. in C/C or C/C-SiC composites. The pyrolysis behavior of phenolic resins is also of great interest when recycling tasks or fire protection measures are under consideration. Cured phenolic resins also have been used as model substrates e. g. to simulate the thermal degradation

of charcoal. The pyrolysis behavior of various carbonaceous materials had been investigated and depicted in so called Van Krevelen Diagramms [7], Fig. 6.

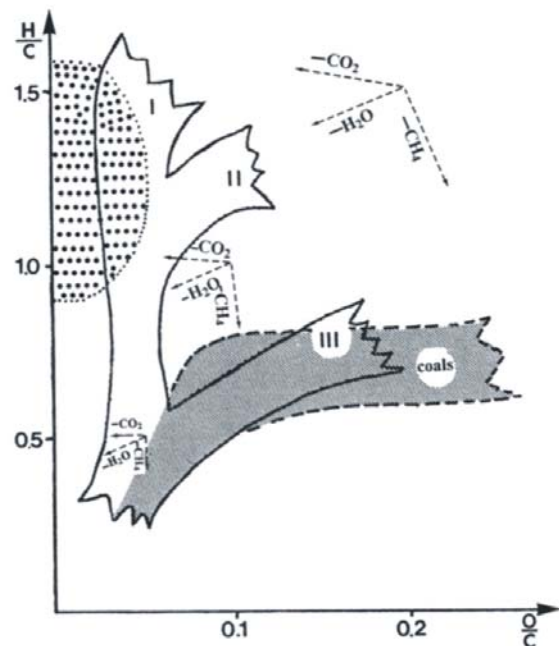


Fig. 6; Van Krevelen Diagramme [7]

These diagrams display empirical knowledge about the graphitizability of carbonaceous materials. Fig. 6 refers to Kerogen and phenolic resins and expresses the finding that the atomar ratios of $H/C < 0,5$ and $O/C > 0,05$ are needed to assure graphitizability. That result coincides with the microstructural model of carbon materials (Fig. 4). Their hydrogen forms a part of the non aromatic cement, which binds together the basic structural units but which is not thermally stable. On the other hand, oxygen serves as a more strong linkage with the result that mobility on the level of the basic structural units, which is required to allow any graphitization, is impeded up to a higher temperature as in case of hydrogen.

The mechanisms of carbonization are not finally clarified. The question, whether the aromatic rings are subjected to a ring opening and renewing processes, is not finally answered. Marker experiments were performed by Cypres [8] and indications for a sub-sequent opening and closing process were found. Whatever is the kinetics, there is no doubt that the existence of aromatic compounds prior to the carbonization is needed and hexagonal basic structural units are produced.

Quantum mechanical calculations are available [2] which correlate microscopic model parameter with macroscopic properties via on electron density distributions with bonding lengths/angles and energies of phenols or some compounds.

2. Experimental

Commercial, state of the art CFRP, C/C and C/C-SiC composites are investigated microstructurally. As their sample history is not known in sufficient detail an own fabrication was installed Fig. 7.

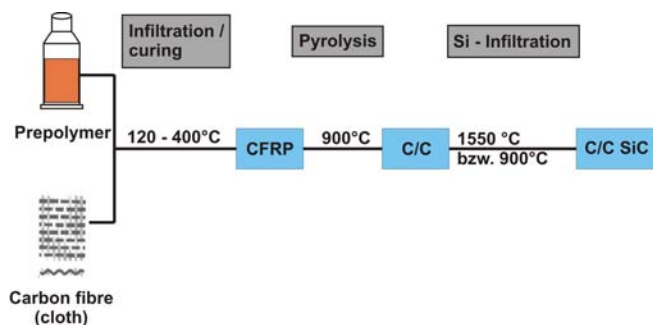


Fig. 7; Fabrication method for CFRP, C/C, C/C-SiC

The Prepolymer (resole) is poured into a small mould which is containing stacked layers of Carbon fibre cloth. Different phenolic resins (raw and modified resins) are used and cured under autoclave conditions (50 bar, $< 180^\circ$) following a reproducible temperature time profile. In the pyrolysis step a muffle type furnace is used under a continuous stream of inert gas (Argon). In the infiltration step high purity Silicon is molten under inert gas on top of the infiltration sample. The infiltration takes place by the capillary effect. Alternatives via plasma activation (high speed infiltration) or vacuum infiltration are tested, too.

The produced samples are subjected to thermogravimetric (TG), a macroscopic-mechanic (DMTA). and microstructural characterization (TEM/FIB).

The FIB/TEM Lift-Out technique [9] is used for a pinpointed and straightforward TEM lamellae preparation

At first the CFRP's matrix porosity and their crack patterns are investigated microscopically (optical microscope, REM and FIB imaging).

The regular pyrolysis process is performed under inert gas (Ar, ambient pressure) in a dedicated muffle type furnace operating under a defined time-temperature profile. Alternatively it is emulated by a time temperature sweeps (RT - 1000 °C, heating rate 4 K/min, Ar, duration approx. 4,5 h) in the Dynamical Mechanical Thermal Analyser (DMTA). In this case the temperature dependence of the Elastic Modulus and of the internal damping ($\tan\delta$) are determined successively starting from the cured CFRP- to the transformed C/C-condition for the different applied matrix.

The evolvement of these materials, which is induced by the pyrolysis process, is traced by REM and TEM and backed by FIB thin film production.

3. Results and Discussion

Microstructural results obtained from commercial materials:

The micrographs show an orthogonal crack system (1. segmentation, Fig. 8a) as an implication of the misfit between matrix shrinkage and the rigid C-fibre reinforcement. Looking closely, the cracks are covered with a porous phase (Fig. 8b) which often contains an open channel inside (Fig. 8c). This leads to the model of a crack according to Fig. 8d. Through these crack the solvent evaporation and the degassing of polymerization products takes place.

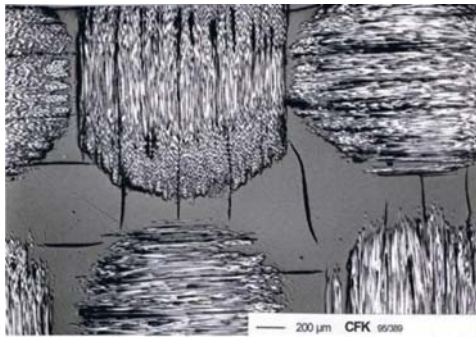


Fig. 8a; CFRP-state, orthogonal crack system

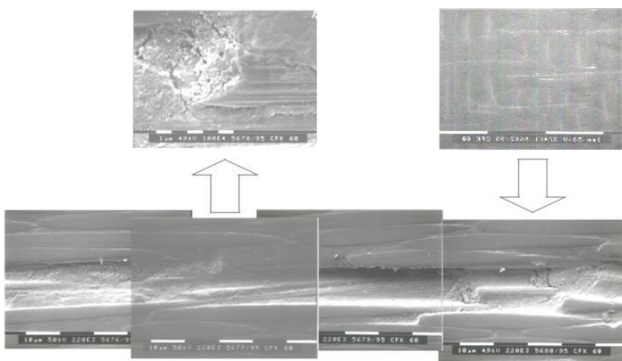


Fig. 8b; porous phase in CFRP formerly covered by a C-fibre

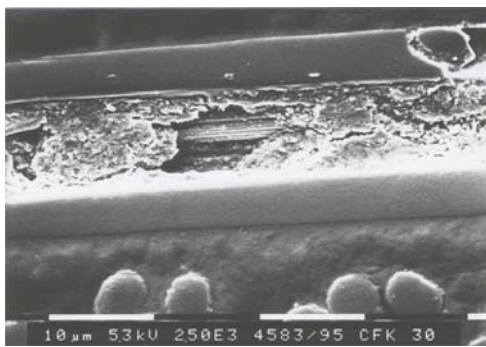


Fig. 8c; gas channel inside porous phase in CFRP

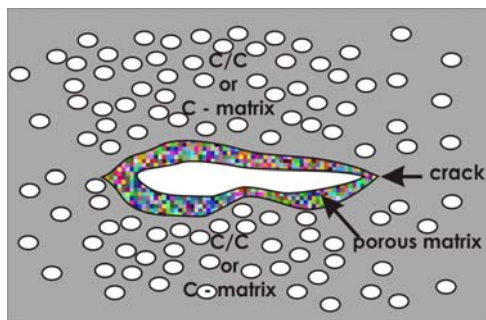


Fig. 8d; artists conception of a crack

The pyrolysis transforms the crack system in a system of zones of reduced C-fibre density (first segmentation) and a finer crack system (second segmentation) which appears to be almost free of foam (Fig. 9a).

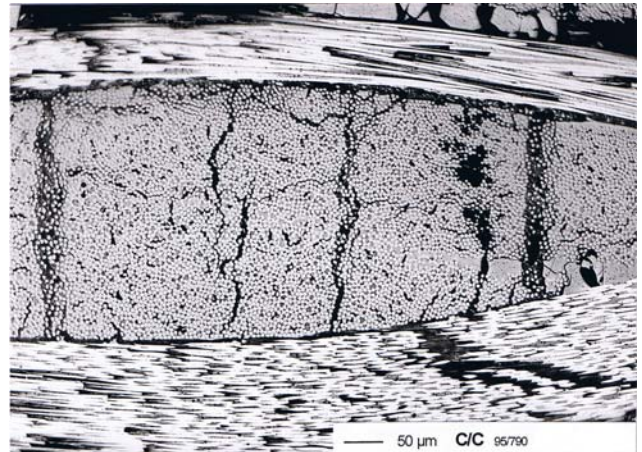


Fig. 9a; C/C-state, 1. and 2. segmentation

In particular the matrix rich areas between differently oriented C-fibre bundles exhibit indications of a locally decrease of the duromeric material state: C-fibre displacements as seen in Fig. 9b.

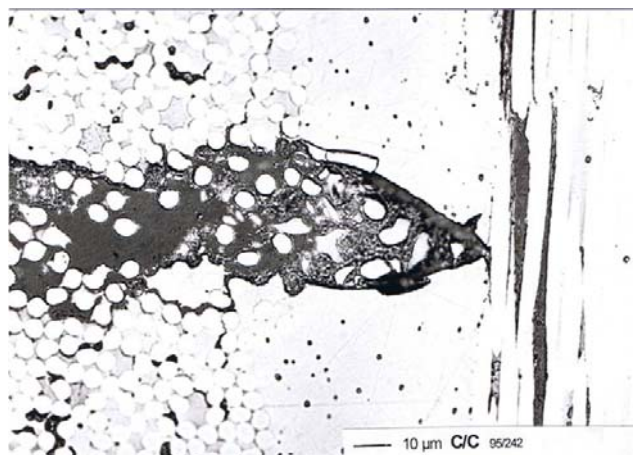


Fig. 9b; filled shrinkage crack, C/C-state

Fig. 9b shows an open gas channel and adjacent porous material inside the crack. This material can be regarded as the pyrolysed porous CFRP phase. But Fig. 9c leads to the assumption that the pyrolysis may also induce recondensation effects. The consistency of the crack phase in Fig. 9c differs significantly from that at several other places of the same sample. All the open channels are suited to transport liquid silicon into the sample (Fig. 10a) by

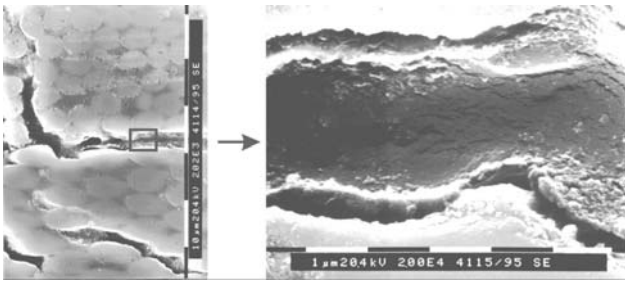


Fig. 9c; porous phase as an indication for an recondensation having occurred

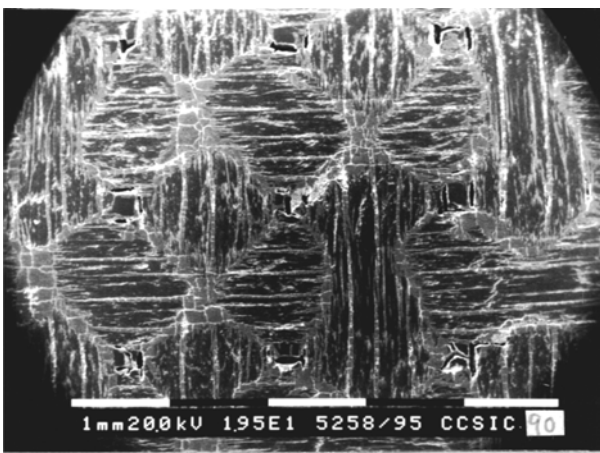


Fig. 10a; C/C-SiC, Si-infiltration into the cracks

the capillary effect. The porous phases act as easily accessible Carbon sources for liquid silicon. After infiltration it reflects to some extent the former crack constitution. In this sense Fig. 10b represents the result of an infiltration of a porous phase which formed a gap to the adjacent more dense materials (locally higher Si concentrations). The former degassing channels appear as areas of elemental

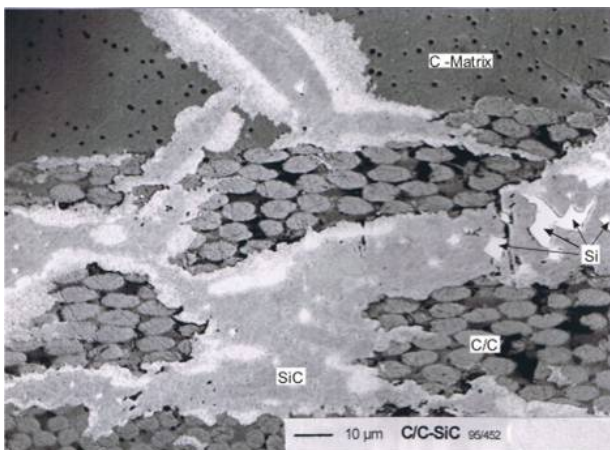


Fig. 10b; typical area in C/C-SiC material

silicon whereas the dense carbon areas slowly degrade by the formation of fine grained β -SiC. TEM analyses reveal the microstructures in the infiltrated cracks more precisely (Fig. 10c). The central crack areas are already consisting of recrystallized β -SiC. They are embedded in fine grained β -SiC, that emerged from the reaction of infiltrated silicon with C-fibres and C-Matrix. In areas where the porous phase is predominant the reaction proceeds much faster and recrystallisation goes ahead. The porous structure of the used T 800 C-fibers (Fig. 10c) shows a reaction ahead of the regular reaction zone. A more detailed investigation of the coarse grained areas leads to the so called β/α -composite crystals [10]. These plate like β/α -composite crystals (Fig. 10d) grow on the expense of the fine grained β -SiC at high temperatures. α -SiC crystals are completely embedded within a thin β -SiC crystal envelope and tend to deteriorate the mechanical properties as investigations of the crack growth and crack propagation indicate. Processing conditions are sought for, which prevent extensive β/α -crystal growth.



Fig. 10c; C/C-SiC; TEM micrograph of a Si-infiltrated crack area



Fig. 10d; β/α -composite crystals in a central crack area

To obtain an impression of the intensity of the pyrolysis and Si-infiltration reactions a video controlled pyrolysis and Si-infiltration was performed. The reaction between C and SiC is such intense that the accompanied gas stream blows out liquid silicon. It seems that a reduction of the reaction speed is indispensable. This experiment was also able to resolve the density change of silicon when solidifying by forming inclined plates.

Further experiments are performed which focus on the Si-reaction time. For these experiments in house fabricated C/C samples were used and the Si-infiltration time is very well controlled. An extremely fast infiltration (PAS-furnace) with a strictly limited Si-infiltration time of 2 minutes (Fig. 11a) was performed and a second series (muffle type furnace) with an extended infiltration time of 8 hours (Fig. 11b). A comparison of the obtained EPMA micrographs shows that the extremely short Si-infiltration (< 2 Min.) can reduce but not prevent the generation of β -SiC. On the other hand a 8 hours infiltration was not sufficient to convert all elemental Si inside the channel to fine grained β -SiC. From this finding it also has to be concluded that the intensive β -SiC recrystallisation as seen in case of the commercial products above needs a longer high temperature exposure time than just 8 hours.

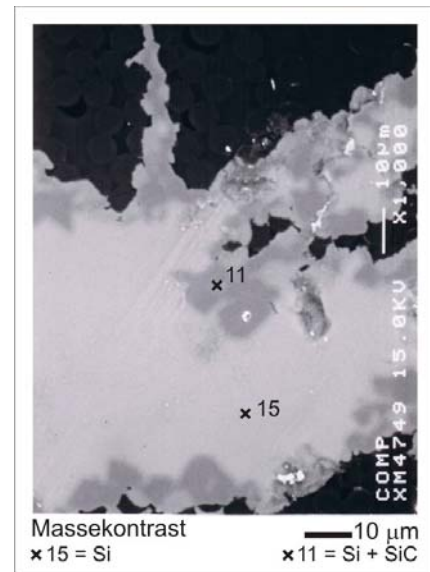


Fig. 11a; High speed Si-infiltration, 2 Min, PAS

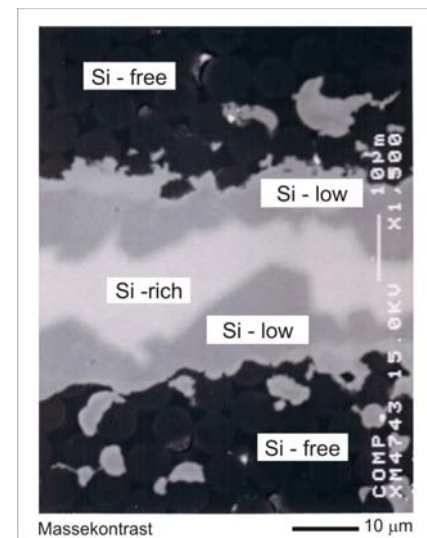


Fig. 11b; Si-infiltration, 8 h, muffle type furnace

More attention was attributed to the microstructure of C-fiber/C-matrix interfaces of in house fabricated C/C composites based on a phenolic resin matrix (E97783, Dynea Erkner GmbH, Germany). In these cases the pinpointed FIB/TEM thin film preparation [9] was applied. It led to a significantly improved thin film quality which even opened nanoscaled pores on both sides at the thin film surface (Fig. 12a) and helped to establish reliable interpretations of the formerly uncertain differences in the observed image contrasts. In case of Fig. 12a the thin film is such thin that along the path of the electron beam through

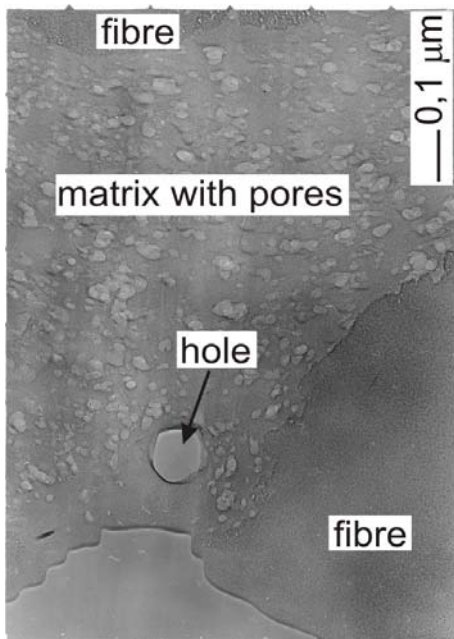


Fig. 12 a; local inter fibre porosity, T800 ox

the film only one or a small number of nano pores are passed, which allows their identification as separated pores. The level of observed closed porosity prevents from regarding it as a dense material. Nevertheless the C-fiber/matrix interface does not show any delaminations.

Being able to display the pores in areas closely adjacent to the C-fibres, the pores serve as indicators of former strains at these areas (Fig. 12. b). They also explain why the composite does not show any indications of stress graphitization: The high level of porosity prevents the generation of sufficiently high stresses to induce the stress graphitization.

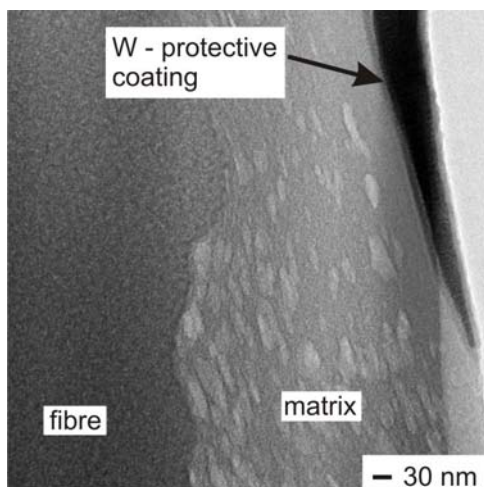


Fig. 12b; pore deformation und local strains, C-fibre type: HTA 5131

The following two micrographs represent two extremal cases of C-fiber/matrix bonding strength. The rough C-fiber of type T800 (Fig. 12c) is known to exhibit a strong C-fiber/matrix bonding strength (e. g. from pull-out tests). The wetting was good; bubbles are always separated by a thin matrix layer from the C-fibre. But also in this case no stress graphitization is observable. Here the rough surface impedes the stress accumulation additionally.

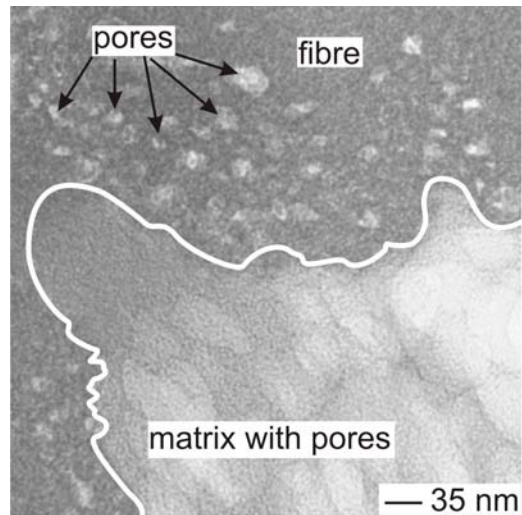


Fig. 12c; C-fibre/C-matrix with significant bonding, C-Fibre type: T800

The reverse case is found in Fig. 12d. Here the C-fiber/matrix bonding strength is low and delamination occurs between C-fiber and matrix even without load. The internal loads are already sufficient. Ex-pitch type carbon fibers usually show low bonding strengths. In case of high modulus ex pitch type C-fibers like YS 90, this effect is most pronounced.

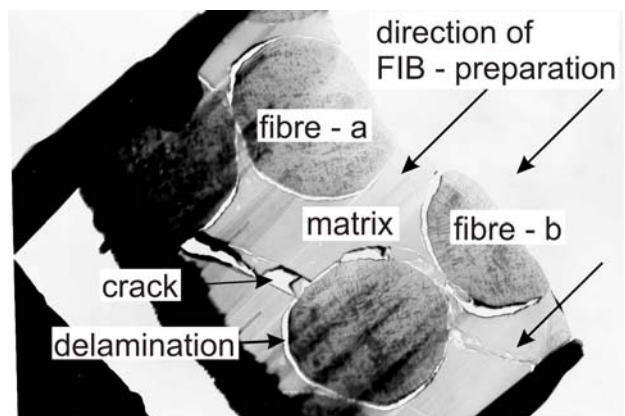


Fig. 12d; C-fibre/C-matrix with very weak bonding C-Fibre type: YS 90

4. Conclusions

The model of phenolic resins according to Hultzsich [1] had been confirmed by combined DMTA and TG investigations, which were performed in parallel. It leads to parameters, which have a potential to influence the resin in early production phases as during the Phenol-Formaldehyde-Addition and during the Prepolymer formation phase.

The advanced FIB/TEM preparation techniques [9] represent valuable tools, which make it possible to display even nano pores reliably and fast.

The performed investigations of porosity on in house fabricated C/C composites succeeded to reveal a microscopical criterium, which represents a reason for the skipped stress graphitization.

Indications for the occurrence of recondensation reactions within the open crack system were found.

The applied experimental methods improve the access to usually hidden micromechanical and structural properties. They still require further investigations of entire polymerization and pyrolysis processes.

5. References

- [1] Hultzsich, K.: Chemie der Phenolharze, Springer-Verlag, Berlin 1950
- [2] Rappoport, Z.(ed.): Phenols - The Chemistry of Phenols, 2 volumes, Wiley 2003
- [3] Haberditzel, W; Scholz, M; Zülicke, L.: Quantenchemie; a series of 3 volumes dedicated to Quantumchemistry, VEB Deutscher Verlag der Wissenschaften, Berlin, 1973, 1981, 1985
- [4] Coulson, C. A.: Die Chemische Bindung; S. Hirzel Verlag, Stuttgart, 1969
- [5] Marsh, H.: Introduction to Carbon Science, ButterworthCo, Ltd., London, 1989
- [6] Oberlin, A.: High Resolution TEM Studies of Carbonization and Graphitization; in: Chemistry and Physics of Carbon, vol. 22, Marcel Dekker Inc., New York, Basel, 1989
- [7] Oberlin, A.; Bonnamy, S.; Rouxhet, P. G.: Colloidal and Supramolecular Aspects of Carbon; in: Chemistry and Physics of Carbon, vol. 26, Marcel Dekker Inc., New York, Basel, 1999
- [8] Cypres, R.; Bettens, B.: Mechanismes de fragmentation pyrolytique du Phenol et des Cresols, Tetrahedron, vol. 30, pp. 1253 - 1260, 1974
- [9] Cypres, R.; Bettens, B.: Pyrolyse Thermique des [¹⁴C] et [³H] ortho et para Cresols, Tetrahedron, vol. 31, pp. 353 - 359
- [9] Cypres, R.; Bettens, B.: La formation de la Plupart des Composes Aromatique produit lors de la Pyrolyse du Phenol, ne fait pas intervenir le Carbone Porteur de la Fonction Hydroxyle, Tetrahedron, vol. 31, pp. 359 - 365, 1975
- [9] Mucha, H., Kato, T, Arai, S. et al.: Focused Ion Beam Prep. Techniques dedicated for the fabrication of TEM lamellae of fibre-reinforced composites, Journal of Electron Microscopy, 54(1), 1 - 7, 2005
- [10] Heuer, A. H.; Fryburg, G. A.; Ogbuji, L. U.; Mitchell, T. E.: $\beta \rightarrow \alpha$ Transformation in Polycrystalline SiC: I, Microstructural Aspects, Journal of the American Ceramic Society, Vol. 61, No. 9-10, pp. 406 - 412, 1978
- [10] Mitchell, T. E.; Ogbuji, L. U.; Heuer, A. H.: $\beta \rightarrow \alpha$ Transformation in Polycrystalline SiC: II, Interfacial Energies, Journal of the American Ceramic Society, Vol. 61, No. 9-10, pp. 412 - 413, 1978
- [10] Ogbuji, L. u.; Mitchell, T. E.; Heuer, A. H.: $\beta \rightarrow \alpha$ Transformation in Polycrystalline SiC: III, The Thickening of α -Plates, Journal of the American Ceramic Society, Vol. 64, No. 2, pp. 91 - 99, 1981
- [10] Ogbuji, L. u.; Mitchell, T. E.; Heuer, A. H.;Shinozaki, S.: $\beta \rightarrow \alpha$ Transformation in Polycrystalline SiC: IV, A Comparison of Conventionally Sintered, Hot-Pressed, Reaction-Sintered and Chemically Vapor-Deposited Samples, Journal of the American Ceramic Society, Vol. 64, No. 2, pp. 100 - 105, 1981